Microstrip differential passband filter with high common-mode suppression using periodically loaded stubs and coupled resonators

Amir Attar, Mojtaba Joodaki

Department of Electrical Engineering, Ferdowsi University of Mashhad, Mashhad, Iran
E-mail: joodaki@um.ac.ir.ir

Published in *The Journal of Engineering*; Received on 25th December 2017; Accepted on 28th January 2018

Abstract: In this study, a periodic structure as a passband filter for differential input signals is introduced that suppresses the common-mode noise with a high common-mode rejection ratio on a wide range of frequencies. The unit cell of the periodic structure consists of open-ended stubs under common-mode and short-ended stubs under differential-mode excitation. The proposed design procedure introduced in this paper can be exploited for different microwave frequency bands while the overall shape of the filter remains unchanged. To verify the design approach, the authors designed and fabricated a filter at the centre frequency of 7 GHz on a Rogers RO4003 substrate with a dielectric constant of 3.7 and a loss tangent of 0.0027. Their studies show that for a three-unit-cell structure with the overall size of 18 mm × 40 mm ($0.75\lambda_g \times 1.66\lambda_g$), a differential fractional bandwidth of 8.6% and a rejection ratio over 55 dB are achieved while the differential in band insertion loss is around 2 dB.

1 Introduction

Common-mode (CM) noise is an unavoidable challenge of microwave circuits and systems. Specially, as the circuits and systems become more complicated and integrated, susceptibility to the environment noise increases. Varieties of methods have been introduced for suppressing CM noise at GHz ranges. These methods are predominantly based on using defected ground structures (DGS) [1–7], CM resonators [8, 9], hybrid multimode resonator and multilayer transitions [10, 11], balance coupled resonators [12–15], stepped impedance resonator (SIR) [16–19], split ring resonator or other metamaterial structures [20–24] and coupled transmission line and stubs [25–30]. On one hand, the efforts are to widen the stopband of CM while decreasing the implementation costs and miniaturising the structures. On the other hand, since bandpass filters (BPFs) are an essential block of RF and communication circuits, several structures are introduced with embedded differential BPFs and CM suppression filters.

In [19], a DGS is used with folded SIR resulting in high selective differential passband filter with enhanced CM suppression. However, DGSs are influenced by the shielded enclosure and its performance is distorted [20]. In [10, 11], multilayer structures that provide wideband differential passband with high CM suppression are introduced, but multilayer filters require more complex and costly fabrication. The two-layer filters based on coupled resonator and SIRs reported in [12–16, 18, 19] are designed at the passband frequencies below 5 GHz. Filters introduced in [25–30] have several benefits such as ultra-wideband and high selective differential passband with low insertion loss; however, they suffer from low CM suppression (<20 dB). In [31], a dual passband filter at higher frequency with improved CM suppression is introduced based on substrate integration waveguide.

According to our best knowledge, this is the first effort to mitigate CM noise on a differential pair based on periodic structures with loaded stubs and coupled resonators. The main aim of this paper is developing a new design approach for such filters. This concept can pave the way for further investigations in this field. Periodic structures have an intrinsic characteristic to filter microwave signals [32]. Although, in theory, the periodic structure is considered to have infinite number of unit-cells, sometimes the desired results can be achieved by cascading a small number of unit cells [32]. For example, in our previous work [33], a three-layer periodic structure with five unit cells is introduced which provides a passband filter with a high CM rejection.

In this work, a design approach based on a novel concept is introduced that can be utilised for any microwave frequency band in which the conventional microstrip technologies can be easily employed in practice. To verify the design concept, some filters with two, three and five unit cells are designed and the one with five unit cells is fabricated. The filter suppresses CM noise in a wide range of frequencies and passes differential signals on a specific passband. In the next section, the idea behind the filter and the design considerations will be discussed. Then, the simulation results including simulated dispersion diagrams and full-wave simulations will be presented. Section 4 covers the measured results and finally, the paper will be concluded in Section 5.

2 Proposed structure

2.1 Principle of operation

A transmission line that is periodically loaded with coupled half-wavelength uniform impedance resonators can be presented by a distributed equivalent circuit with a single unit-cell as depicted in Fig. 1. The unit cell consists of an admittance π circuit in the middle and two equal transmission lines on the left and right sides. The electrical length of the unit cell is equal to a quarter of guided wavelength, $\lambda_g/4$, i.e. the phase shift along the unit cell is $kP = \theta = \pi/2$, in which k is the wave number of the unloaded line and P is the unit-cell's length. According to Fig. 1 and assuming $g = P$, the transmission matrix can be derived as [32]

$$\boldsymbol{M} = \begin{bmatrix} \cos\frac{\theta}{2} & j\sin\frac{\theta}{2} \\ j\sin\frac{\theta}{2} & \cos\frac{\theta}{2} \end{bmatrix} \times \begin{bmatrix} 1+\frac{y_1}{y_2} & \frac{1}{y_2} \\ 2y_1+\frac{(y_1)^2}{y_2} & 1+\frac{y_1}{y} \end{bmatrix} \times \begin{bmatrix} \cos\frac{\theta}{2} & j\sin\frac{\theta}{2} \\ j\sin\frac{\theta}{2} & \cos\frac{\theta}{2} \end{bmatrix} = \begin{bmatrix} A & B \\ C & D \end{bmatrix} \quad (1)$$

doi: 10.1049/joe.2017.0903

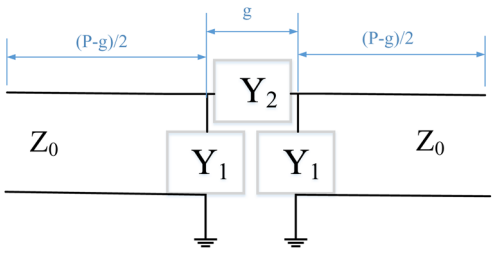

Fig. 1 *Unit-cell equivalent circuit for a transmission line periodically loaded with reactive elements with physical length of P*

Assuming a θ very close to $\pi/2$, A, B, C and D can be reduced to

$$A = D = \frac{1}{2}j\left(2y_1 + \frac{(y_1)^2}{y_2} + \frac{1}{y_2}\right) \tag{2a}$$

$$B = j\left(1 + \frac{y_1}{y_2}\right) + \frac{1}{2}\left(\frac{1}{y_2} - 2y_1 - \frac{(y_1)^2}{y_2}\right) \tag{2b}$$

$$C = j\left(1 + \frac{y_1}{y_2}\right) + \frac{1}{2}\left(2y_1 + \frac{(y_1)^2}{y_2} - \frac{1}{y_2}\right) \tag{2c}$$

where y_1 and y_2 are lossless admittances normalised by the characteristic admittance of the line, Y_0. Assuming that $y_1 = jb_1$ and $y_2 = jb_2$, dispersion relation of the periodic structure can be expressed as

$$\begin{aligned}\cos \beta P = \frac{(A+D)}{2} = A &= \frac{1}{2}j\left(2jb_1 + j\frac{(b_1)^2}{b_2} - j\frac{1}{b_2}\right) \\ &= 1 - (b_1+1)\left(1 + \frac{(b_1-1)}{2b_2}\right)\end{aligned} \tag{3}$$

In order to have stopband or passband, proper values of b_1 and b_2 should be chosen. The normalised susceptance of b_2 which is a gap capacitance is a positive value between 0 and 1 ($0 < b_2 < 1$) at the frequency range of interest. If b_1 is chosen as $|b_1| < 1 - 2b_2$, right side of (3) becomes >1 and a stopband will be guaranteed. However, by choosing b_1 near -1, right side of (3) might have a value between -1 and 1, which causes a passband.

By employing a pair of half-wavelength resonators, the signal can be transmitted through the unit cell at the resonance frequency while having the required short circuits and open circuits near the signal line. This can generate a small positive b_1 for CM noise and a b_1 near -1 for the desired differential mode (DM) signal. The input admittances of open circuit stub (Y_{OC}) and short circuit stub (Y_{SC}) are [32]

$$Y_{OC}(l) = jY_0' \tan(\beta' l) \tag{4a}$$

$$Y_{SC}(l) = -jY_0' \cot(\beta' l) \tag{4b}$$

where l, β' and Y_0' are the length, the propagation constant and the characteristic admittance of the stubs, respectively. With a proper impedance matching and due to the unit-cell symmetry, the signals at the coupled lines at each side of the unit-cell symmetry plane have a similar phase which causes an even-mode coupling. Thus, β' and Y_0' are the even-mode propagation constant and characteristic admittance of the coupled lines, respectively.

The proposed structure is a differential pair of microstrip line consisting of five unit cells that the top layer of which is depicted in Fig. 2. A split with size of g in the centre of each unit cell forms a gap capacitance. The differential lines are connected together at both sides of the split. These interconnects with the length of S and the width of t form both the coupled half-wavelength resonators and the required stubs at the resonance

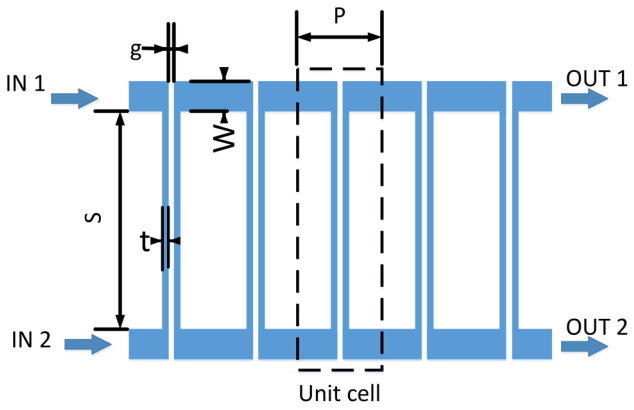

Fig. 2 *Top layer of the proposed filter structure*

frequency (short circuit stubs for the DM excitation and the open circuit stubs for the CM excitation). Therefore, the stubs' length (l) is equal to $S/2 - \lambda_g'/2$ (see Fig. 3). The width of the differential pair lines is equal to W and P is the length of the unit cells. By selecting a proper S, the desired conditions will be guaranteed. The symmetric line between the differential pair is a virtual perfect electric conductor for the DM and a virtual perfect magnetic conductor for the CM excitations.

2.2 Design procedure

As already mentioned, under CM excitation, $|b_1|$ should be $< 1 - 2b_2$. Considering (4a), this can be achieved if the length of l is small enough. Hence, $S/2$ is chosen to be a bit longer than $\lambda_g'/2$ and numerical value of b_1 under CM excitation can be derived from

$$b_1^d = \frac{Y_0'}{Y_0} \tan(\beta^{d\prime} l) \tag{5}$$

Under DM excitation, b_1 should be near -1. Moreover, due to the length of l, the short-ended stubs cause large admittance values. However, by minimising the ratio of the line admittances to stubs admittances, i.e. Y_0'/Y_0, b_1 will be near -1. Numerical value of b_1 under DM excitation can be obtained from

$$b_1^c = -\frac{Y_0'}{Y_0} \cot(\beta^{c\prime} l) \tag{6}$$

Applying (3) and assuming a negative value of b_1, lower and upper cut-off frequencies are as follows, respectively:

$$f_L = \frac{c}{S\sqrt{\varepsilon'_{reff}}}\left(1 + \frac{1}{\pi}\tan^{-1}\left(\frac{Y_0'}{Y_0}\frac{1}{1+2b_2}\right)\right) \tag{7a}$$

$$f_H = \frac{c}{S\sqrt{\varepsilon'_{reff}}}\left(1 + \frac{1}{\pi}\tan^{-1}\left(\frac{Y_0'}{Y_0}\right)\right) \tag{7b}$$

in which c is the speed of light in free space and ε'_{reff} is the effective relative permittivity. From (7a) and (7b), the desired band can be determined. Additionally, Bloch impedance of the structure is [32]

$$Z_B = \frac{BZ_0}{\sqrt{A^2 - 1}} = \frac{b_1^d + b_2 - ((b_1^d)^2 + 2b_1^d b_2 + 1)}{\sqrt{(b_2)^2 - (1 - (b_1^d)^2 - 2b_1^d b_2)}} \tag{8}$$

The design procedure can be shortened in four steps:

(i) Assuming an initial value for the design respective to the centre frequency of the band.
(ii) Making sure that $b_1^e < 1 - 2b_2$.

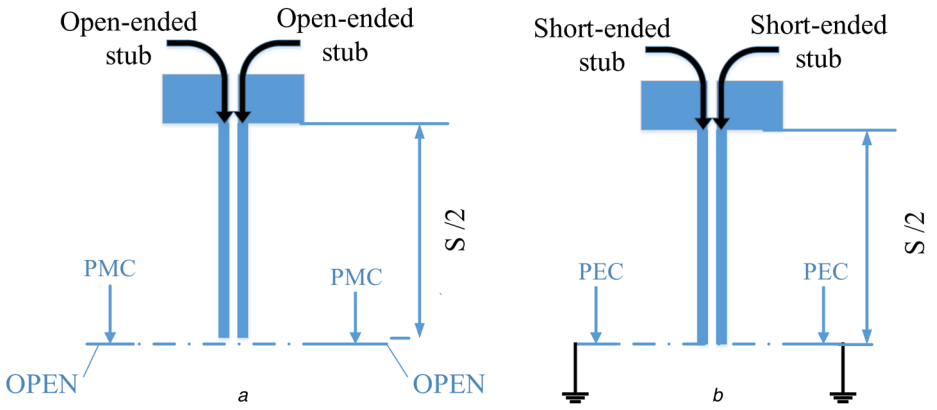

Fig. 3 *Stubs created by the vertical lines*
a Under CM excitation
b Under DM excitation

(iii) Choosing proper values for S, the ratio of (Y_0'/Y_0) and b_2 to create the desired band, according to (7a) and (7b).
(iv) Using (8), re-evaluating b_1^d and b_2 so that Z_B and the port impedance are matched.

Since in each step, the parameters cannot be independently set, a simple iteration approach is needed to evaluate the parameters in steps (ii)–(iv). Therefore, by selecting reasonable initial values and after a few iterations, a desired band with the minimum reflection (S_{dd11}) can be obtained.

3 Simulation results and discussion

Based on the concept described in the last section, a filter, as a prototype, is designed with a centre frequency of 7 GHz and fractional bandwidth of 8.6%. By assuming a P near a quarter of the guided wavelength and sweeping the other design parameters, the best S_{dd12} (DM transmission) is achieved. The optimised parameters are $W=3$, $S=28$, $t=0.2$, $g=0.2$ and $P=6$ mm. With these dimensions, the gap capacitance is 0.3 pF, $\lambda_g=24$ mm, $\lambda_g'=27.2$ mm, $Y_0=0.041$ S and $Y_0'=0.0135$ S.

The dispersion relations of the filter with infinite numbers of unit cells have been simulated by HFSS for both CM and DM propagations. As is shown in Fig. 4, β_{common} remains zero over all of the frequency range. This means there is a cut-off for CM propagation around the centre frequency. Under DM excitation, however, there is a passband between 6.5 and 7.5 GHz. In addition, three-dimensional full-wave electromagnetic simulation of the structure has been performed by using HFSS.

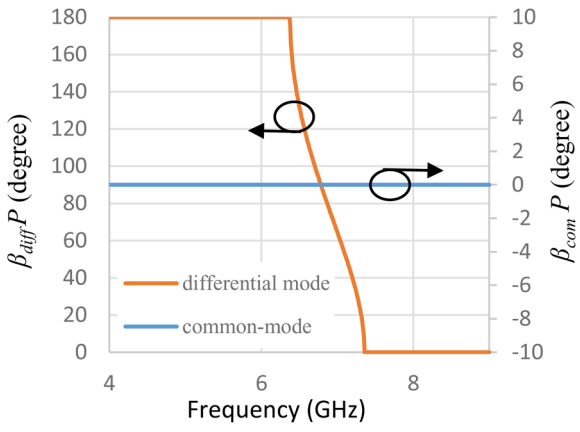

Fig. 4 *Dispersion diagrams for DM and CM propagations*

As predicted from the dispersion diagrams, CM signal is rejected by a suppression level larger than 60 dB.

As mentioned before, this method of design can be applied to different microwave frequency bands only through modification of the design parameters while not changing the overall structure shape. This means that by using the previously introduced design steps, the desired bandpass can be achieved in different frequency bands. If the structure is scaled homogeneously, the bandpass decreases proportional to the scaling factor with the same Fractional Bandwidth (FBW). This is due to the fact that the ratio of Y_0'/Y_0 remains constant by scaling of the structure [34]. In addition, although b_2 is affected by changing the dimensions, as it is very smaller than 1, its variation does not have a considerable effect. Thus, according to (7a) and (7b), f_L and f_H are inversely proportional to S. Furthermore, the Bloch impedance, according to (8), shows a different behaviour and scaling the structure would degrade the matching. However, for scaling factors between 0.5 and 2, the filter almost retains at the same Bloch impedance. The prototype filter is designed for centre frequency of 7 GHz and it is scaled by factors of 2, 0.7 and 0.5. In order to perform the scaling, all parameters of W, S, t, h, p and g are simply multiplied by the scaling factor.

As is shown in Fig. 5, the centre frequency of the differential bandpass varies inversely by the scaling factor and occurs in 3.5, 10 and 14 GHz, respectively. Although the matching is good at 10 GHz, in 3.5 and 14 GHz it is degraded. However, their in-band S_{dd11} are still lower than −15 dB. Therefore, the scaled structure is an appropriate initial solution and it can be easily optimised by following the design steps in Section 2 to obtain an acceptable matching. It should be noted that only the filter with 7 GHz centre frequency is numerically optimised in this work and the scaled designs are used with no further tuning.

On one hand, in-band insertion loss of the differential signal is proportional to the number of unit cells due to the discontinuities along the signal's path. On the other hand, the common suppression improves as the number of the unit cells increases. Thus, there is a trade-off between CM suppression level and in-band differential insertion loss. As it is depicted in Fig. 6, for a bigger number of unit cells, both CM suppression and in-band insertion loss would increase.

4 Experimental results

In order to obtain a high CM suppression, a five-unit-cell structure is fabricated with the centre frequency of 7 GHz. The overall size of the filter is 30 mm × 40 mm, equal to $1.25\lambda_g \times 1.66\lambda_g$ where λ_g is guided wavelength at the centre frequency of the differential passband. The substrate used is a 20-mil-thick Rogers RO4003C PCB with a relative dielectric constant of 3.7 and a loss

doi: 10.1049/joe.2017.0903

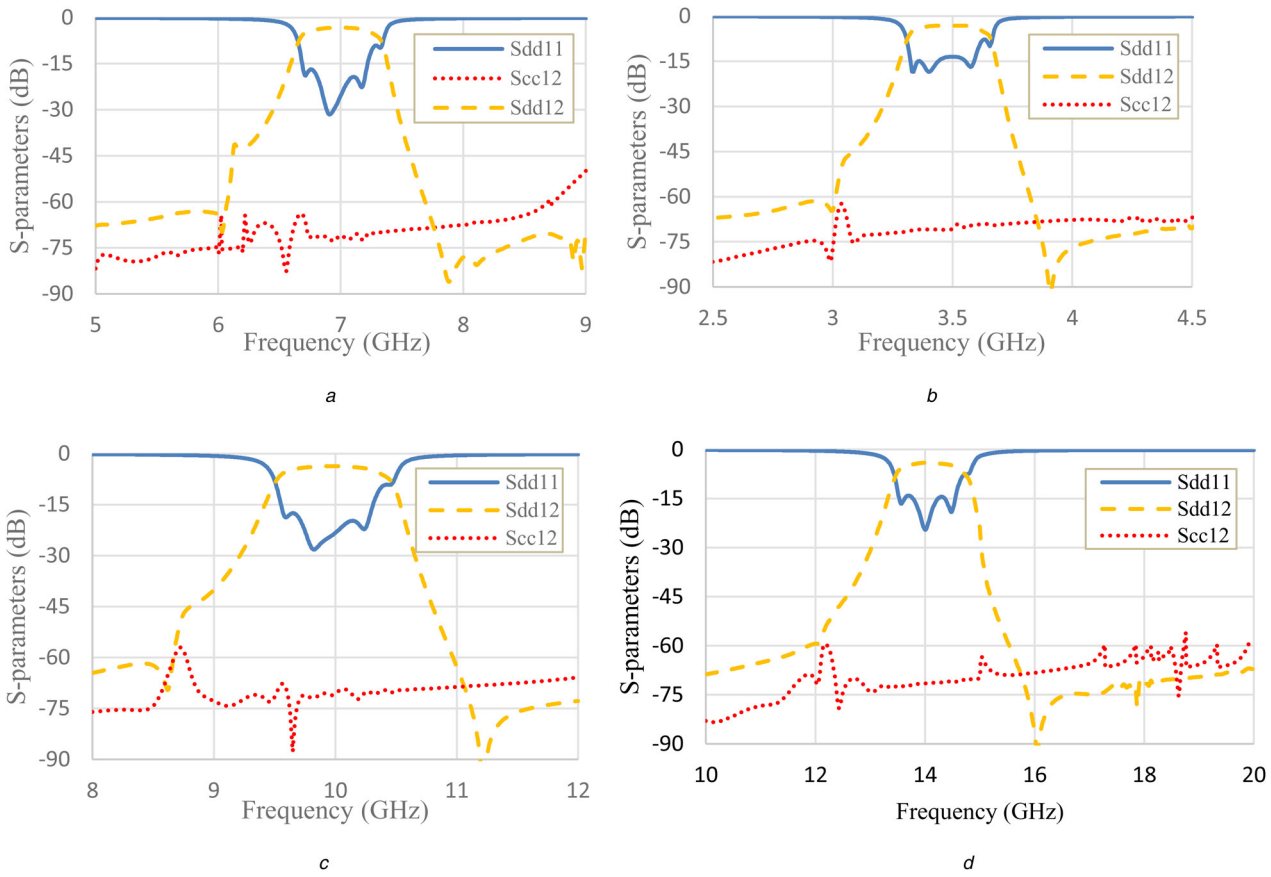

Fig. 5 *Simulated S-parameters*
a Original prototype
b Filter scaled by a factor of 2
c Filter scaled by a factor of 0.7
d Filter scaled by a factor of 0.5

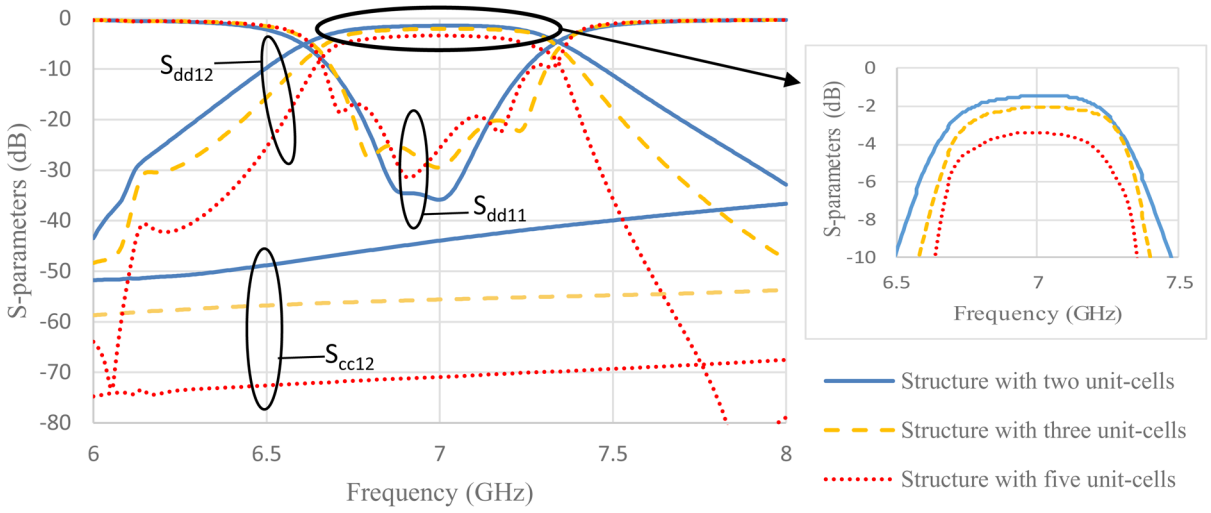

Fig. 6 *Comparison of simulated results of insertion loss and CM suppression of the structures with two, three and five unit cells*

tangent of 0.0027. The photograph of the fabricated filter is shown in Fig. 7. Ports 1 and 3 form the differential input while the differential output is established by ports 2 and 4. Using an Agilent PNA-E8363B and two 50 Ω loads, single-mode *S*-parameters for four ports are measured. Then, the single-mode measurements are converted to the mixed mode *S*-parameters.

Fig. 8 shows the simulation and experimental results of the DM and CM signal's propagations through the filter in frequency range of 5–9.5 GHz. The CM suppression is over 60 dB and the differential passband is at the centre frequency of 7 GHz with FBW of 8.6%. In fact, the CM suppression is limited by imperfections in the PCB fabrication process and the measurement facilities.

Fig. 9 demonstrates the simulated and measured in-band differential insertion and reflection losses. In-band insertion loss is 3.5 dB in simulated results and 3.7 dB in measurement results. Both simulated and measured differential reflection losses are lower than

doi: 10.1049/joe.2017.0903

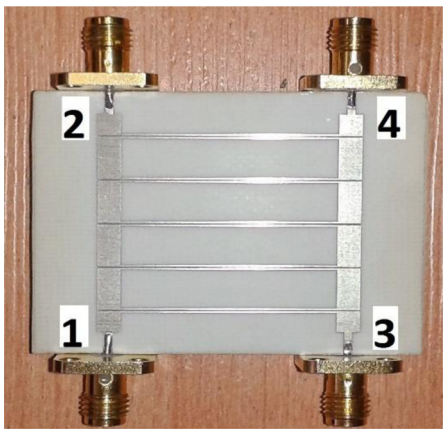

Fig. 7 *Photograph of the fabricated five unit cells filter*

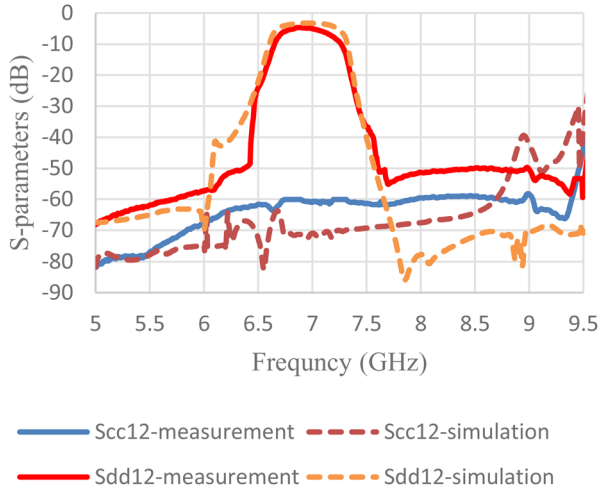

Fig. 8 *CM and DM S-parameters*

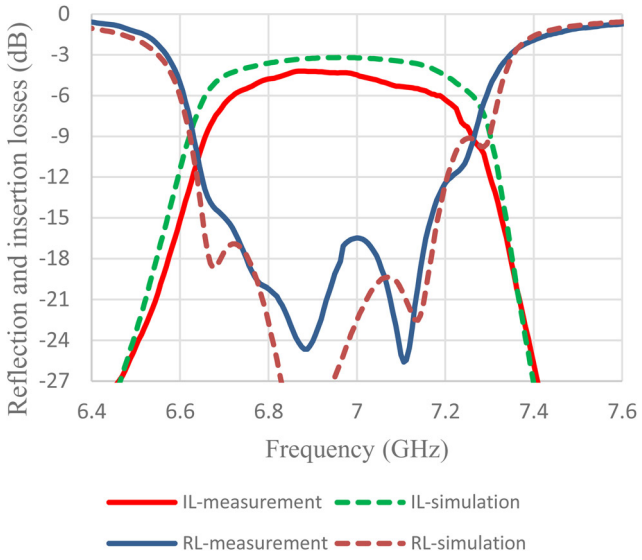

Fig. 9 *Reflection and insertion losses of the differential signal in the passband*

−15 dB which shows a good consistency between the simulation and the measurement results. In Table 1, our results are compared with those of some two-layer structures previously published in the literature. The highest CM suppression is achieved in our filter with five unit cells. Even our filter with three unit cells provides a CM suppression more than 55 dB with only <2 dB in-band differential insertion loss.

Table 1 Results of our work in comparison with those of some previous works

Ref	f_{0d}, GHz	FBW, %	In-band IL, dB	CM suppression in the DM passband, dB	Size ($\lambda_g \times \lambda_g$)
[15]	2.93	6.9	2	30	0.21 × 0.2
[16]	2.45	9.8	2.55	25	0.41 × 0.37
[19]	2.5	10	1.57	34	0.15 × 0.21
[24]	1	10	2.8	25	0.1 × 0.25
[29]	2.49	8	2.64	51	1 × 0.14
this work, three unit cells	7	8.6	2	55	0.75 × 1.66
this work, five unit cells	7	8.6	3.7	60	1.25 × 1.66

5 Conclusion

An embedded differential passband and CM suppression filter based on periodic structures, in which the unit-cell consists of a π circuit and two equal transmission lines, is introduced. The shunt elements of the π circuit are $\lambda/2$-type resonators that provide short-circuit stubs under DM excitations and open-circuit stubs under CM excitations. This causes a passband for differential signals and a stopband for CM signals. Design steps described in this paper can be utilised for other frequency bands, too. Easy design, simple structure, via-free layout, low cost implantation and high CM rejection level over a wide range of frequencies are the main benefits of our filter.

6 Acknowledgments

The authors thank all members of the EMI/EMC and Microwave Technology Research Laboratory at Department of Electrical Engineering, Ferdowsi University of Mashhad, Mashhad, Iran for their help and support.

7 References

[1] Wu S.-J., Tsai C.-H., Wu T.-L., *ET AL.*: 'A novel wideband common-mode suppression filter for gigahertz differential signals using coupled patterned ground structure', *IEEE Trans. Microw. Theory Tech.*, 2009, **57**, (4), pp. 848–855

[2] Liu W.T., Tsai C.H., Han T.W., *ET AL.*: 'An embedded common-mode suppression filter for Ghz differential signals using periodic defected ground plane', *IEEE Microw. Wirel. Compon. Lett.*, 2008, **18**, (4), pp. 248–250

[3] Lin D.B., Lee Y.H.: 'A wideband common-mode suppression filter using enhanced coupled defected ground structure'. 2016 IEEE Int. Symp. on Electromagnetic Compatibility (EMC), 2016

[4] Zhu H.R., Mao J.F.: 'An ultra-wideband common-mode suppression filter based on S-dbcsrr for high-speed differential signals', *IEEE Microw. Wirel. Compon. Lett.*, 2015, **25**, (4), pp. 226–228

[5] Shi Y., Zhuang W., Wang C., *ET AL.*: 'Common-mode suppression design for gigahertz differential signals based on coupled C-slotlines'. 2015 Asia-Pacific Microwave Conf. (APMC), IEEE, 2015

[6] Choi J.H., Hon P.W., Itoh T.: 'Dispersion analysis and design of planar electromagnetic bandgap ground plane for broadband common-mode suppression', *IEEE Microw. Wirel. Compon. Lett.*, 2014, **24**, (11), pp. 772–774

[7] Vélez P., Naqui J., Fernández-Prieto A., *ET AL.*: 'Ultra-compact (80) differential-mode ultra-wideband (Uwb) bandpass filters with common-mode noise suppression', *IEEE Trans. Microw. Theory Tech.*, 2015, **63**, (4), pp. 1272–1280

[8] Liu Q., Li G., Khilkevich V., *ET AL.*: 'Common-mode filters with interdigital fingers for harmonics suppression and lossy materials for broadband suppression', *IEEE Trans. Electromagn. Compat.*, 2015, **57**, (6), pp. 1740–1743
[9] Shiue G.-H., Hsu C.-M., Yeh C.-L., *ET AL.*: 'A comprehensive investigation of a common-mode filter for gigahertz differential signals using quarter-wavelength resonators', *IEEE Trans. Compon., Packag. Manuf. Technol.*, 2014, **4**, (1), pp. 134–144
[10] Guo X., Zhu L., Wu W.: 'Balanced wideband/dual-band bpfs on a hybrid multimode resonator with intrinsic common-mode rejection', *IEEE Trans. Microw. Theory Tech.*, 2016, **64**, (7), pp. 1997–2005
[11] Shi J., Shao C., Chen J.-X., *ET AL.*: 'Compact low-loss wideband differential bandpass filter with high common-mode suppression', *IEEE Microw. Wirel. Compon. Lett.*, 2013, **23**, (9), pp. 480–482
[12] Olvera-Cervantes J.-L., Corona-Chavez A.: 'Microstrip balanced bandpass filter with compact size, extended-stopband and common-mode noise suppression', *IEEE Microw. Wirel. Compon. Lett.*, 2013, **23**, (10), pp. 530–532
[13] Wu C.-H., Wang C.-H., Chen C.H.: 'Balanced coupled-resonator bandpass filters using multisection resonators for common-mode suppression and stopband extension', *IEEE Trans. Microw. Theory Tech.*, 2007, **55**, (8), pp. 1756–1763
[14] Wu C.-H., Wang C.-H., Chen C.H.: 'Novel balanced coupled-line bandpass filters with common-mode noise suppression', *IEEE Trans. Microw. Theory Tech.*, 2007, **55**, (2), pp. 287–295
[15] Chen D., Zhu L., Bu H., *ET AL.*: 'Differential-mode bandpass filter on microstrip line with wideband common-mode suppression', *Electron. Lett.*, 2017, **53**, (3), pp. 163–165
[16] Lee C.-H., Hsu C.-I.G., Hsu C.-C.: 'Balanced dual-band Bpf with stub-loaded sirs for common-mode suppression', *IEEE Microw. Wirel. Compon. Lett.*, 2010, **20**, (2), pp. 70–72
[17] Chu H., Li P., Chen J.-X.: 'Balanced substrate integrated waveguide bandpass filter with high selectivity and common-mode suppression', *IET Microw. Antennas Propag.*, 2015, **9**, (2), pp. 133–141
[18] Shi J., Xue Q.: 'Dual-band and wide-stopband single-band balanced bandpass filters with high selectivity and common-mode suppression', *IEEE Trans. Microw. Theory Tech.*, 2010, **58**, (8), pp. 2204–2212
[19] Fernández-Prieto A., Martel J., Medina F., *ET AL.*: 'Compact balanced fsir bandpass filter modified for enhancing common-mode suppression', *IEEE Microw. Wirel. Compon. Lett.*, 2015, **25**, (3), pp. 154–156
[20] Tsai C.-H., Wu T.-L.: 'A broadband and miniaturized common-mode filter for gigahertz differential signals based on negative-permittivity metamaterials', *IEEE Trans. Microw. Theory Tech.*, 2010, **58**, (1), pp. 195–202
[21] Naqui J., Fernandez-Prieto A., Duran-Sindreu M., *ET AL.*: 'Common-mode suppression in microstrip differential lines by means of complementary split ring resonators: theory and applications', *IEEE Trans. Microw. Theory Tech.*, 2012, **60**, (10), pp. 3023–3034
[22] Velez P., Naqui J., Fernández-Prieto A., *ET AL.*: 'Differential bandpass filter with common-mode suppression based on open split ring resonators and open complementary SplitRing resonators', *IEEE Microw. Wirel. Compon. Lett.*, 2013, **23**, (1), pp. 22–24
[23] Velez P., Bonache J., Martın F.: 'Dual-band balanced bandpass filter with common-mode suppression based on electrically small planar resonators', *IEEE Microw. Wirel. Compon. Lett.*, 2016, **26**, (1), pp. 16–18
[24] Horestani A.K., Durán-Sindreu M., Naqui J., *ET AL.*: 'S-Shaped complementary split ring resonators and their application to compact differential bandpass filters with common-mode suppression', *IEEE Microw. Wirel. Compon. Lett.*, 2014, **24**, (3), pp. 149–151
[25] Wu X.-H., Chu Q.-X.: 'Compact differential ultra-wideband bandpass filter with common-mode suppression', *IEEE Microw. Wirel. Compon. Lett.*, 2012, **22**, (9), pp. 456–458
[26] Li L., Bao J., Du J.-J., *ET AL.*: 'Compact differential wideband bandpass filters with wide common-mode suppression', *IEEE Microw. Wirel. Compon. Lett.*, 2014, **24**, (3), pp. 164–166
[27] Wu X.-H., Chu Q.-X., Qiu L.-L.: 'Differential wideband bandpass filter with high-selectivity and common-mode suppression', *IEEE Microw. Wirel. Compon. Lett.*, 2013, **23**, (12), pp. 644–646
[28] Li L., Bao J., Du J.-J., *ET AL.*: 'Differential wideband bandpass filters with enhanced common-mode suppression using internal coupling technique', *IEEE Microw. Wirel. Compon. Lett.*, 2014, **24**, (5), pp. 300–302
[29] Jiang W., Peng Y., Shen W., *ET AL.*: 'Dual-mode dual-band balanced filter with high differential-mode frequency selectivity and enhanced common-mode suppression'. 2015 IEEE MTT-S Int. Microwave Symp., IEEE, 2015
[30] Lim T.B., Zhu L.: 'Highly selective differential-mode wideband bandpass filter for Uwb application', *IEEE Microw. Wirel. Compon. Lett.*, 2011, **21**, (3), pp. 133–135
[31] Shen Y., Wang H., Kang W., *ET AL.*: 'Dual-band Siw differential bandpass filter with improved common-mode suppression', *IEEE Microw. Wirel. Compon. Lett.*, 2015, **25**, (2), pp. 100–102
[32] Pozar D.M.: 'Microwave engineering' (J. Wiley, New York, USA, 2005)
[33] Attar A., Joodaki M.: 'A wide differential passband filter with common-mode suppression property based on left handed metamaterial transmission line'. Int. Symp. on Electromagnetic Compatibility (EMC EUROPE), 2016
[34] Wadell B.C.: 'Transmission line design handbook' (Artech House, Boston, USA, 1991)